

Fast random rewiring and strong connectivity impair subthreshold signal detection in excitable networks

Vladislav Volman^{1,2,4} and Matjaž Perc³

¹ Center for Theoretical Biological Physics, University of California at San Diego, La Jolla, CA 92093, USA

² Computational Neurobiology Laboratory, The Salk Institute for Biological Studies, La Jolla, CA 92037, USA

³ Department of Physics, Faculty of Natural Sciences and Mathematics, University of Maribor, Koroška cesta 160, SI-2000 Maribor, Slovenia
E-mail: volman@salk.edu

New Journal of Physics **12** (2010) 043013 (11pp)

Received 12 November 2009

Published 1 April 2010

Online at <http://www.njp.org/>

doi:10.1088/1367-2630/12/4/043013

Abstract. We study dynamical responses in locally paced networks consisting of diffusively coupled excitable units with dynamically adjusted connectivity. It is shown that for weak subthreshold pacing, excessive or strong connectivity impairs the reliable response of a network to the stimulus. Fast random dynamic rewiring of the network also acts detrimentally on signal detection by enforcing a faster relaxation upon the paced unit. Our results indicate that efficient signal processing on excitable complex networks requires tight correspondence between the dynamics of connectivity and the dynamical processes taking place on the network. This, in turn, suggests the existence of ‘function-follows-form’ principles for systems described within this framework.

Contents

1. Introduction	2
2. The model and methods of analysis	3
3. Results	6
4. Discussion	10
Acknowledgments	10
References	10

⁴ Author to whom any correspondence should be addressed.

1. Introduction

Excitability is an important property of several biological and artificial systems, ranging from neural networks and cardiac tissue to chemical reaction systems and laser optics [1–4]. Weak perturbations acting upon an excitable steady state typically evoke spiking responses, which after a system-characteristic refractory time fade anew towards the steady state. Excitations can be triggered by stochastic or deterministic inputs, whereby one can observe fascinating phenomena such as, for example, stochastic and coherence resonance in temporal and spatially extended systems [5–9], pattern formation and firing synchronization [10] or self-sustained activity [11] and fast coherent responses [12] in small-world neural networks, to mention but a few. Indeed, especially in neural systems, excitability plays a pivotal role and remains an inspiration for ongoing research efforts, as evidenced by recent focus issues devoted to this subject [13, 14]. For example, the excitability of so-called leader neurons has been found crucial for the development of bursts of activity in neural networks [15]. Inspired by preceding experimental observations [16], it was conjectured that the leader neurons form a sub-network that acts as a nucleation area for the bursts upon its initial excitation.

Although the majority of studies has so far considered static networks or has dealt with the network architecture and connection strengths in a probabilistic fashion [17], the focus has recently been shifting towards evolving or adaptive networks [18]. In particular, evolving or dynamically changing interactions in the context of excitable neural networks have been considered previously by Bazhenov *et al* [19], who examined the role of network dynamics in shaping spike timing reliability. Also, Levina *et al* [20, 21] reported on the existence of self-organized criticality due to dynamical synapses in a pulse-coupled neural network, while coherence resonance due to rewiring has been presented recently by Jiang and Ma [22] in the context of diffusively coupled FitzHugh–Nagumo neurons. Outside the realm of excitable systems, Mondal *et al* [23] showed that the rapid switching of random links among chaotic maps enhances spatiotemporal regularity of their dynamics. Moreover, synchronization on evolving complex networks has also been studied. Sorrentino and Ott [24] proposed an adaptive strategy based on defining an appropriate potential that each node aims to minimize, and it was shown that a similar technique could be used for adaptive learning of a time-evolving network topology as well [25]. Following these developments, further studies examined the emergence of synchronization on evolving complex networks [26, 27] and were subsequently integrated into the broader scope of synchronization on complex networks, as reviewed comprehensively in [28].

Our motivation here is to extend the scope of the above studies and gain an understanding about how the connectivity structure of a network of excitable units could contribute to various aspects of signal processing. We focus on a network's detection of weak periodic signals in the framework of small-world architecture and try to understand how some features of connectivity, such as the fraction of shortcuts between the excitable nodes, determine the ability of a network as a whole to detect the signal that is introduced to one of its units (i.e. the paced unit). We show that connectivity and topology can have counterintuitive effects on signal detection in locally paced networks. Namely, we show that excessively strong connectivity of the paced unit impairs reliable signal detection, and we provide a theoretical argument to explain this effect. We then consider the effect that random dynamic redistribution of connectivity has on the ability of a locally paced network to detect a weak localized stimulus, and we demonstrate that fast random rewiring reduces the response of a network. Our observations suggest that the optimal

strategy for weak signal detection in locally paced networks of diffusively coupled excitable units should be tightly linked to activity-dependent rewiring of the connectivity. This, in turn, suggests a practical realization of the ‘function-follow-form’ principle [29–33] on evolving networks, whereby the structure (or form) of the network defines its function, in this case being the dynamical response to the weak signal.

The paper is structured as follows. In section 2, we describe the employed mathematical model, as well as the interaction networks and other mathematical methods presently in use. The results are presented in section 3. In the last section, we summarize our findings and discuss their potential implications.

2. The model and methods of analysis

We consider networks of diffusively coupled excitable units, with network topology ranging from practically regular to random. The temporal evolution of the i th unit (time is discretized in our model as an iteration number) is described by the following set of map equations that were developed to capture the rich variety of neuronal dynamics, from regular spiking to self-sustained chaotic bursting [34, 35]

$$u_i(t+1) = \frac{\alpha}{1+u_i^2(t)} + v_i(t) + D \sum_{j=1}^N \varepsilon_{ij} [u_j(t) - u_i(t)] + \sigma \xi(t), \quad (1)$$

$$v_i(t+1) = v_i(t) - \beta u_i(t) - \gamma.$$

In equation (1), the variable u_i captures the fast component of neural dynamics, whereas v_i evolves on a slower time scale. The parameter D represents the strength of diffusive coupling between the given unit and the set of its ‘neighbors’ (parameterized by the matrix ε_{ij}), which consists of both the unit’s neighbors on the regular lattice and of contributions that come from shortcut links to randomly picked units, constructed as detailed below. For the sake of clarity, we assume that the strength of the coupling D is the same for all pairs of coupled units. Elements of matrix ε_{ij} take the following values:

$$\varepsilon_{ij} = \begin{cases} 1 & : i, j \text{ connected,} \\ 0 & : i, j \text{ not connected.} \end{cases} \quad (2)$$

In this work, we consider networks with structures ranging from almost regular, through small-world, to almost randomized. We start from the ring-like network with regular connectivity, where each unit is coupled to its nearest neighbor on each side of the ring. Then, for each pair of previously unconnected units, the shortcut connection is established with the probability p_s . The value of p_s determines the topological characteristics of the network (the averaged minimal path length between the units and the clustering coefficient).

In addition to being coupled to the rest of the network, each of the units is subject to temporally and spatially uncorrelated Gaussian noise $\xi(t)$, with intensity σ invariant across the network and not dependent on time, such that

$$\langle \xi_i(t) \xi_j(t + \Delta t) \rangle = \sigma^2 \delta(\Delta t) \delta_{ij}. \quad (3)$$

The goal of the present study is to understand the effects that dynamic changes in the network’s connectivity have on the collective population-wide response to weak local stimulation. To this

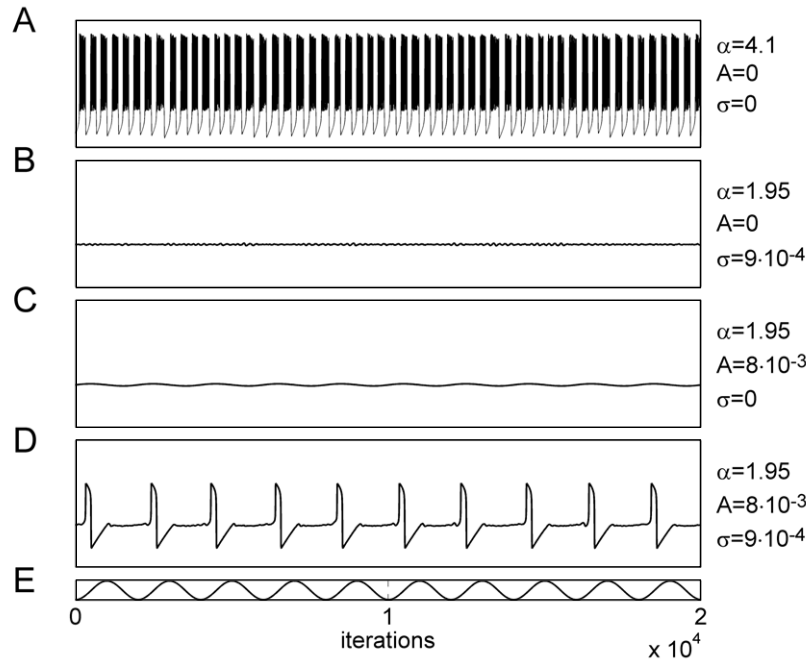


Figure 1. Dynamical behavior of the nonlinear map model used in this study. (a) Dynamics of the model for $\alpha = 4.1$. In this regime, the map exhibits self-sustained chaotic bursts in the absence of any external stimulation ($A = 0$, $\sigma = 0$). (b), (c) In the excitable regime ($\alpha = 1.95$), neither noise alone (in the absence of the signal, (b)) nor the signal alone (in the absence of noise, (c)) are able to evoke spiking. (c) Only the application of both, the signal and noise, results in the detection of the otherwise subthreshold signal. (d) Signal trace. In all panels the results were obtained on a single map unit, i.e. not coupled to any other units.

end, one of the units is stimulated by a weak periodic signal $I_{\text{app}}(t)$ with frequency f and amplitude A

$$I_{\text{app}}(t) = A \sin(2\pi ft), \quad (4)$$

which is added to the dynamics of variable u . Depending on the values of its parameters, the map model can exhibit different dynamical behaviors [34]. For example, for sufficiently high α (as in figure 1(a), where $\alpha = 4.1$) an individual map can exhibit self-sustained chaotic bursts that do not require external inputs ($\sigma = 0$ and $A = 0$). To work in the excitable regime, we set $\alpha = 1.95$. It is important to note that in the excitable regime that we consider here, neither the Gaussian noise (parameterized by σ) nor the signal (parameterized by f and A) alone is supra-threshold, i.e. the spiking activity of the paced unit occurs only when both the noise and the signal are applied to it, as depicted in figures 1(b)–(e). Even for the joint application of noise and signal, however, the response of the coupled paced unit is quite irregular (the coherence of spiking (see equation (5)) is less than 1) and depends on the coupling strength between the units and on the abundance of shortcut connections (figure 2(c)). Parameter values used throughout this work are $\beta = \gamma = 0.001$ and $\alpha = 1.99$. Initially, all units are initialized

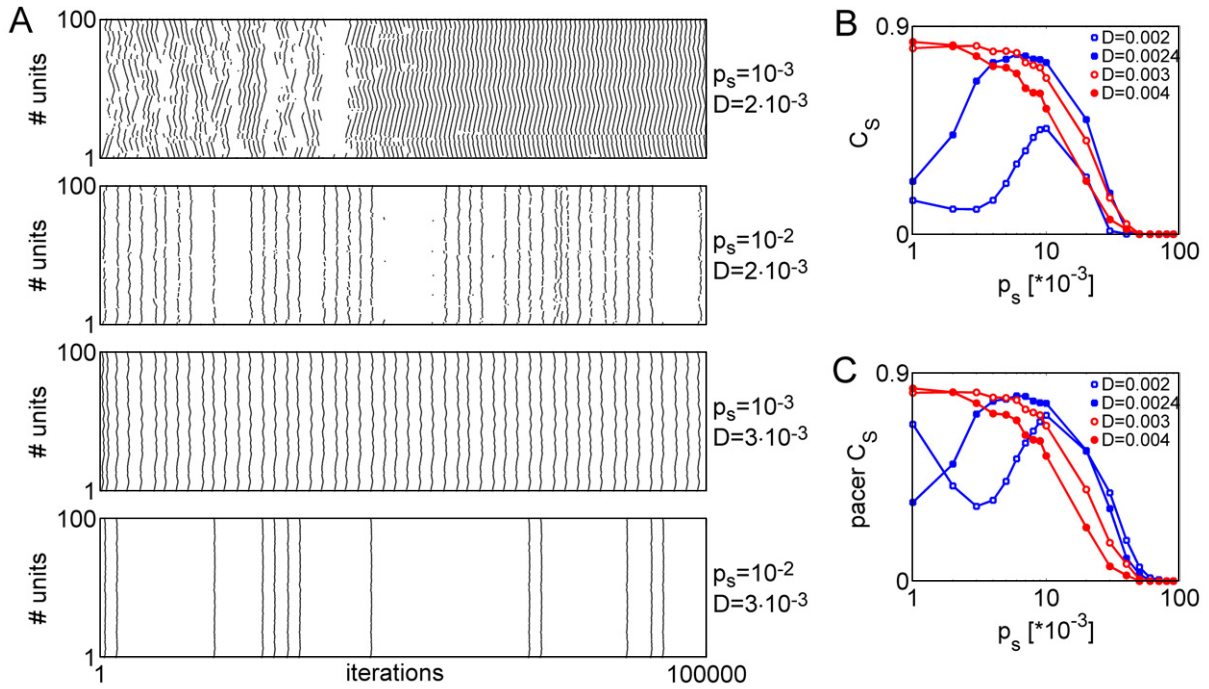


Figure 2. The collective response of excitable networks to the weak localized stimulus. (a) Raster plots of network activity showing the response for different coupling strengths D and abundance of shortcuts p_s . Top panel: $p_s = 10^3$ and $D = 2 \times 10^{-3}$. The second panel: $p_s = 10^{-2}$ and $D = 2 \times 10^{-3}$. The third panel: $p_s = 10^{-3}$ and $D = 3 \times 10^{-3}$. Bottom panel: $p_s = 10^{-2}$ and $D = 3 \times 10^{-3}$. (b) Network-averaged coherence of spiking C_S versus the probability of shortcut connection p_s for different values of the coupling strength D . Data points are averages over 100 independent realizations. (c) Coherence of spiking C_S solely of the paced unit versus the probability of shortcut connections p_s for different values of the coupling strength D . Data points are averages over 100 independent realizations.

from the fixed point of equation (1), which for $\alpha < 2$ (and $D = 0$, $\sigma = 0$) is given by $u^* = -1$ and $v^* = -1 - (\alpha/2)$. In what follows, and unless otherwise specified, we used $\sigma = 9 \times 10^{-3}$, $A = 8 \times 10^{-3}$ and $f = 5 \times 10^{-4}$ (in units 1/iteration).

In the setting described above, the ability of a single excitable unit to detect weak periodic stimuli can be conveniently quantified by using the so-called ‘coherence of spiking’ measure [36]. The coherence of spiking measure C_S is defined as a fraction of interspike intervals (ISI) that are within 20% of the stimulus period T :

$$C_S = \frac{N(\text{ISI} | 0.9T \leq \text{ISI} \leq 1.1T)}{N(\text{ISI})}. \quad (5)$$

Unless otherwise indicated, the measure given by equation (5) is computed for each excitable unit individually and then the average is taken over all of the units in the network and over a large number (typically 100) of statistically independent realizations.

3. Results

A brief glance at the network's raster plots (figure 2(a)) suggests that the pattern of collective activity that develops in the network in response to weak pacing does strongly depend on the structure of the network. Both the strength of the coupling (parameterized by D) and the connectivity (parameterized by p_s) can critically affect the collective dynamics. Visual inspection confirms that there might exist an optimal level of coupling strength and fraction of shortcut links that maximize the coherent response to the periodic pacing stimulation. This is in agreement with earlier observations [37, 38]. We note, however, that interesting phenomena can be observed when either the coupling is made relatively strong (compare the top and second panels in figure 2(a)) and/or the number of shortcut links is relatively high (compare the top and third panels in figure 2(a)); in either of these cases, naive reasoning would imply that the activity has to be more intense (as a result of stronger coupling and a more connected network), but the actual outcome is exactly the opposite. Thus, in the studied excitable network, the relative contribution of strong coupling and strong connectivity can determine the efficiency with which the weak subthreshold signal is detected. The goal of this work is to elucidate the mechanisms responsible for this counterintuitive effect brought about by the network connectivity and coupling strength.

To quantify the above qualitative observations regarding the effects of coupling and connectivity, we use here the simple measure of output coherence relative to the input signal periodicity. For periodic stimulation, this coherence measure C_S is defined as a fraction of the element's interspike intervals that fall within the 20% window of the stimulation period T (see equation (5)). Figure 2(b) shows the dependence of averaged output-to-input coherence on the fraction of shortcut links in the excitable network, for different levels of the coupling strength. Two features are eminent. Firstly, coherence of the network's response falls to zero in the large p_s limit (corresponding to a strongly wired network with randomized topology). Secondly, stronger coupling between the units increases the C_S only up to a certain value of the coupling strength, and the effect of increased coupling on the coherence depends on the fraction of shortcut links p_s (figure 2(b)). From these observations it follows that there exists a coupling-dependent range of p_s values, for which the network is optimally coherent with the weak subthreshold signal that is introduced to the paced unit. This can indeed be observed in figure 2(b) (open squares and closed squares). Since the networks we study are locally paced, it is of interest to examine the signal detection properties of the paced unit as well. In figure 2(c), we show the output–input coherence of the paced unit activity, plotted for different scenarios of the network's connectivity and the coupling strength. The striking difference between the paced unit response (figure 2(c)) and the averaged response of the whole network (figure 2(b)) is evident in the limit of low p_s and weak coupling ($D = 0.002$)—the activity of the paced unit is highly coherent with the input signal, but this is not the case for the activity of other units. Thus, in the limit of weak connectivity and coupling, signal detection is reliable, but signal propagation is not.

Why does the network exhibit low coherence to input when the wiring and/or coupling are excessively strong? In principle, the reduced coherence could be either the outcome of some intrinsic alternation in network dynamics or it could arise because of the reduced ability of the pacer to detect the weak signal. The results shown in figures 2(b) and (c) suggest that the latter cause might hold. To understand the role played by the paced unit, we examine the dynamics of networks for which the paced unit was spared from getting any shortcut connections (it was

only connected to its nearest neighbors on the regular lattice). Figure 3(a) (top) shows that this modified network is coherent to input over a much wider range of p_s than was the baseline model network. This enhanced response is a direct result of an enhanced response of the paced unit (the bottom panel of figure 3(a)). A more detailed investigation (controlling the level of the paced unit's connectivity to the rest of the network) reveals that the values of C_S for the paced element fall sharply as the number of its nearest neighbors (and/or the strength of the coupling to them) is increased (the top left panel of figure 3(c)), and this kind of behavior could be attributed to the smaller number of spikes that the pacer generated in a fixed time interval (the bottom left panel of figure 3(c)). Consistent with this, a change in the signal's amplitude leads to a change in the coherence-connectivity relation of the paced element (right panels of figure 3(c)). However, as the weaker coupling of the paced element increases its coherence with the input signal, the reduced ability to relay the stimulus-related information to other elements results in a decrease of averaged network coherence. This is evident from figure 3(d), where we show the averaged C_S of the paced unit's neighbors versus the coherence of that same paced unit. We conclude that the network's coherence in the strong coupling/wiring limit becomes low because of the feedback from the network to the paced element that reduces the latter's ability to detect the signal. This is similar to the dependence of rheobase currents on related parameters in models of gap junction-coupled neuronal ensembles. Thus, in the currently studied excitable system, having non-uniform connectivity, the network's architecture in itself determines its propensity to respond to a subthreshold signal. This complements and extends (to some extent) some of the earlier results (although for a different network model) that showed how signal properties determine the ability of a network to detect the signal [39].

We now offer an explanation for the degrading effect that the strong connectivity and/or strong coupling have on the coherent response to the subthreshold stimulus. In networks of diffusively coupled units, we can rewrite the coupling term in equation (1) as

$$D \sum_{j=1}^N \varepsilon_{ij} [u_j(t) - u_i(t)] = \sum_{j=1}^N \varepsilon_{ij} \frac{u_j(t) - u_i(t)}{D^{-1}}. \quad (6)$$

Therefore, the coupling between the units can be looked at as a linear relaxation term (assuming the coupling coefficient is constant). The relaxation time τ_R of the coupling is inversely proportional to the strength of coupling; therefore stronger coupling enforces faster relaxation of weak perturbations in the dynamics of the paced unit, thus impairing its response to the subthreshold stimulus (figure 3(c)). By the same token, higher connectivity (higher p_s) also acts to decrease the coupling-related relaxation time and thus also acts to impair the subthreshold signal detection (figure 3(c)).

Recently, increasing theoretical [23, 24] and experimental [40] effort has been devoted to understand the effects that dynamic rewiring of network connectivity might have on its dynamics. In particular, for the small-world modeling framework, it has been shown that various dynamic properties (such as the propensity to synchronize) can depend on the rate with which shortcut connections are rewired [24]. In another study [23], it was shown that fast dynamic rewiring could bring about the spatiotemporal order into an otherwise chaotic network. We anticipated that in the currently studied excitable network, dynamic rewiring of shortcuts could have strong effects by virtue of its redefining the effective connectivity of the paced unit. Figure 4(a) demonstrates the dependence of C_S on the fraction of shortcut links, for different rates of random shortcut rewiring and different strengths of coupling between the units.

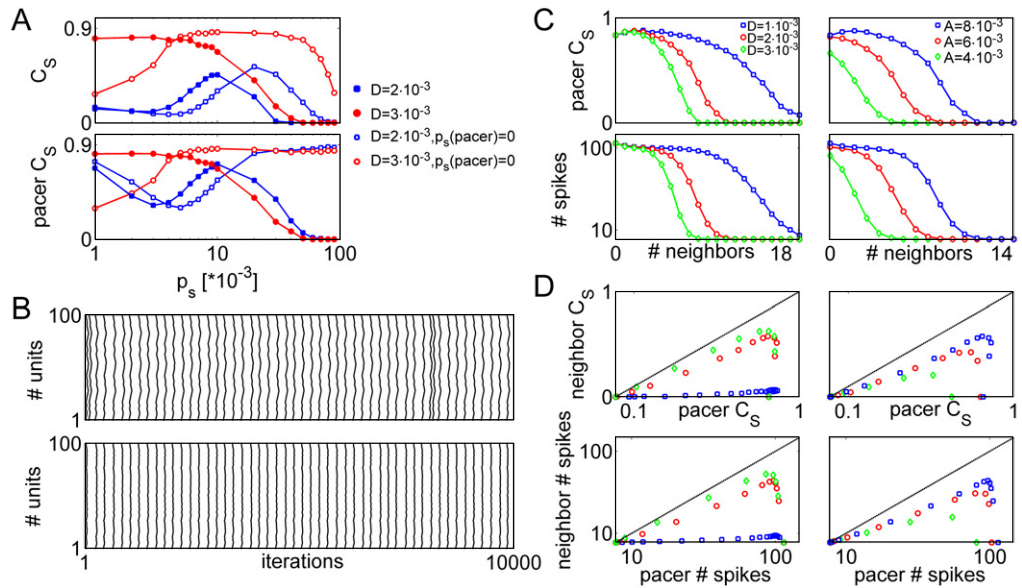


Figure 3. Strong connectivity of the paced excitable unit impairs reliable detection of subthreshold signals. (a) Network-averaged (top panel) and paced unit's (bottom panel) coherence of spiking C_S versus the probability of having shortcut connections p_s for different values of the coupling strength D , as indicated by blue squares and red circles. Closed symbols are for the baseline model. Open symbols are for the modified model in which the paced unit is not allowed to establish shortcut connections with other units. All data points are averages over 100 independent realizations. (b) Raster plots of the network's activity showing the response for $D = 3 \times 10^{-3}$, $p_s = 10^{-3}$ (top panel) and $D = 3 \times 10^{-3}$, $p_s = 10^{-2}$ (bottom panel). In both cases, the paced unit was not allowed to establish shortcut connections with other units. (c) Top left: coherence of spiking C_S solely of the paced unit versus its connectivity for different values of D . Bottom left: number of spikes fired by the paced unit in the window of 2×10^5 iterations versus its connectivity for different values of D (as in top left). Top right: coherence of spiking C_S of the paced unit versus its connectivity for different amplitudes of the weak signal (coupling strength was fixed at $D = 2 \times 10^{-3}$). Bottom right: number of spikes fired by the paced unit in the window of 2×10^5 iterations versus its connectivity for different amplitudes of the weak signal (as in top right). All data points are averages over 100 independent realizations. (d) Top left: neighbor-averaged (average over all neighbors of the paced unit) coherence of spiking versus the C_S of solely the paced unit for different values of D (as in top left of (c)). Bottom left: neighbor-averaged number of spikes versus the number of spikes fired by the paced unit for different values of D (as in bottom left of (c)). Top right: neighbor-averaged coherence of spiking versus the C_S of solely the paced unit for different values of A (as in top right of (c)). Bottom right: neighbor-averaged number of spikes versus the number of spikes fired by the paced unit for different values of A (as in bottom right of (c)). In all the panels, the dashed line denotes slope 1, while all data points are averages over 100 independent realizations.

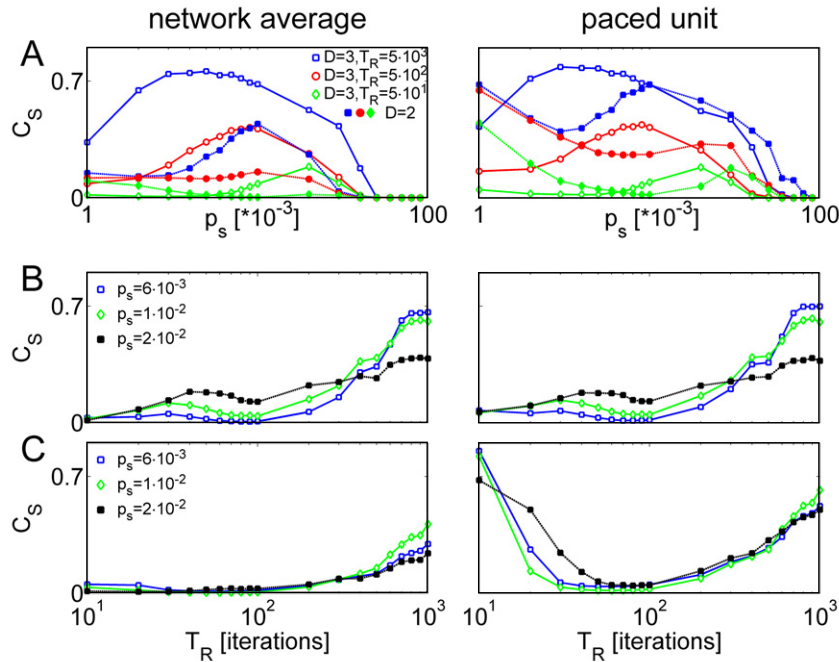


Figure 4. Fast random rewiring of the network impairs reliable detection of subthreshold signals. (a) Network-averaged (left panel) and paced unit's (right panel) coherence of spiking C_S versus the probability of having shortcut connections p_s for different values of the shortcuts rewiring time: $T_R = 5 \times 10^3$ (blue squares), $T_R = 5 \times 10^2$ (red circles) and $T_R = 5 \times 10^1$ (green diamonds). Open symbols depict results for $D = 3 \times 10^{-3}$. The corresponding closed symbols depict results for $D = 2 \times 10^{-3}$. All data points are averages over 100 independent realizations. (b) Network-averaged (left panel) and paced unit's (right panel) coherence of spiking C_S versus the rewiring time of shortcuts for different levels of shortcut abundance probability: $p_s = 6 \times 10^{-3}$ (open blue squares), $p_s = 1 \times 10^{-2}$ (open green diamonds) and $p_s = 2 \times 10^{-2}$ (closed black squares). The strength of coupling between the units is $D = 3 \times 10^{-3}$. All data points are averages over 100 independent realizations. (c) Network-averaged (left panel) and paced unit's (right panel) coherence of spiking C_S versus the rewiring time of shortcuts for different levels of shortcut abundance probability: $p_s = 6 \times 10^{-3}$ (open blue squares), $p_s = 1 \times 10^{-2}$ (open green diamonds) and $p_s = 2 \times 10^{-2}$ (closed black squares). The strength of coupling between the units is $D = 2 \times 10^{-3}$. All data points are averages over 100 independent realizations.

The generic effect of fast rewiring is to decrease the coherence of output activity with respect to the input signal. In networks with dynamically rewired shortcuts, the effective shortcut connectivity p_s^* of each unit is $P_S^* \approx P_S T_R^{-1}$, where T_R is the period (measured in terms of the number of iterations) with which the shortcut links are rewired [23]. Thus, either fast shortcut rewiring or the abundant presence of fixed shortcuts increases the effective connectivity and, according to our explanation, impairs the subthreshold signal detection by the paced unit. A tangential observation is that the level of p_s for which the peak coherence is observed scales inversely with the rewiring time T_R (figures 4(b) and (c)).

4. Discussion

Several recent studies indicate that dynamic rewiring of interactions among units can have important consequences for the organization of activity in networks of excitable units. Here, we have investigated the effects of dynamic connectivity rewiring on the properties of subthreshold signal detection in locally paced networks of diffusively coupled excitable units. Quite counterintuitively, excessively strong connectivity and/or excessively strong coupling was found to impair subthreshold signal detection. This negative effect of connectivity occurred because stronger coupling enforced a faster relaxation on the dynamics of the paced unit, thus reducing its response to the weak stimulus. Consistent with these ‘static’ effects, fast dynamic rewiring also acted detrimentally on the collective response of the network to the weak stimulus.

The collective response of a locally paced network to the weak stimulus consists of two stages. Firstly, the stimulus has to be locally detected, and secondly, it needs to be quickly and efficiently relayed to the rest of the network. In the networks studied here, fast random rewiring of connectivity impaired the collective reaction of the system to the weak subthreshold stimulus. This raises an interesting question—what should be the rewiring strategy so as not to compromise either one of the stages (detection or transmission of the input) in signal processing? Clearly, the rewiring has to depend in some way on the pattern of ongoing activity, i.e. render the network with adaptive features. This is reminiscent of activity-dependent redistribution of connectivity in neural networks and is consistent with the idea of the reciprocal function–form (dynamics–structure) relation. That is, the form (structure) determines the function (dynamics), which in turn affects the form (structure). It remains to be investigated what are the dynamical rules that give rise to optimal signal detection in diffusively coupled networks of excitable units.

The presented results might improve our understanding of the dynamics of weak signal detection and propagation in diffusively coupled excitable networks, such as networks of neurons or astrocytes (a type of glial cells) coupled by diffusive gap junctions [41]. In modeling studies, the connectivity of these networks is usually assumed to be regular (constant number of gap junctions per neuron/astrocyte); however, in reality the distribution of gap junction connectivity is quite broad [42]. How does this broad connectivity, and the emerging heterogeneity of the network’s architecture [43], affect signal processing in such biological networks is a question that seems worth exploring in the future by using more specific models.

Acknowledgments

VV acknowledges support from the NSF-sponsored Center for Theoretical Biological Physics (grant number PHY-0822283 to Herbert Levine). MP acknowledges support from the Slovenian Research Agency (grant number Z1-2032).

References

- [1] Zykov V S 1987 *Simulation of Wave Processes in Excitable Media* (Manchester: Manchester University Press)
- [2] Winfree A T 2000 *The Geometry of Biological Time* (Berlin: Springer)
- [3] Lindner B, García-Ojalvo J, Neiman A and Schimansky-Geier L 2004 *Phys. Rep.* **392** 321
- [4] Izhikevich E M 2007 *Dynamical Systems in Neuroscience: The Geometry of Excitability and Bursting* (Cambridge, MA: MIT Press)

- [5] Jung P and Mayer-Kress G 1995 *Phys. Rev. Lett.* **74** 2130
- [6] Pikovsky A S and Kurths J 1997 *Phys. Rev. Lett.* **78** 775
- [7] Longtin A and Chialvo D R 1998 *Phys. Rev. Lett.* **81** 4012
- [8] Gammaitoni L, Hänggi P, Jung P and Marchesoni F 1998 *Rev. Mod. Phys.* **70** 223
- [9] Sagués F, Sancho J M and García-Ojalvo J 2007 *Rev. Mod. Phys.* **79** 829
- [10] Wang Q Y, Duan Z S, Huang L, Chen G R and Lu Q S 2007 *New J. Phys.* **9** 383
- [11] Roxin A, Riecke H and Solla S A 2004 *Phys. Rev. Lett.* **92** 198101
- [12] Lago-Fernández L F, Huerta R, Corbacho F and Sigüenza J A 2000 *Phys. Rev. Lett.* **84** 2758
- [13] Bodenschatz E and Wolf F 2008 *New J. Phys.* **10** 015002
- [14] Arecchi F T and Kurths J 2009 *Chaos* **19** 015101
- [15] Eckmann J-P, Jacobi S, Marom S, Moses E and Zbinden C 2008 *New J. Phys.* **10** 015011
- [16] Eytan D and Marom S 2006 *J. Neurosci.* **26** 8465
- [17] Rabinovich M I, Varona P, Selverston A I and Abarbanel H D I 2006 *Rev. Mod. Phys.* **78** 1213
- [18] Gross T and Blasius B 2008 *J. R. Soc. Interface* **5** 259
- [19] Bazhenov M, Rulkov N F, Fellous J M and Timofeev I 2005 *Phys. Rev. E* **72** 041903
- [20] Levina A, Herrmann J M and Geisel T 2007 *Nat. Phys.* **3** 857
- [21] Levina A, Herrmann J M and Geisel T 2009 *Phys. Rev. Lett.* **102** 118110
- [22] Jiang M and Ma P 2009 *Chaos* **19** 013115
- [23] Mondal A, Sinha S and Kurths J 2008 *Phys. Rev. E* **78** 066209
- [24] Sorrentino F and Ott E 2008 *Phys. Rev. Lett.* **100** 114101
- [25] Sorrentino F and Ott E 2009 *Phys. Rev. E* **79** 016201
- [26] Hagberg A and Schult D A 2008 *Chaos* **18** 037105
- [27] De Lellis P, di Bernardo M and Garofalo F 2008 *Chaos* **18** 037110
- [28] Arenas A, Díaz-Guilera A, Kurths J, Moreno Y and Zhou C 2008 *Phys. Rep.* **469** 93
- [29] Towle V L, Carder R K, Khorasanil L and Lindberg D 1999 *J. Clin. Neurophysiol.* **16** 528
- [30] Hilgetag C C, Burns G A, O'Neill M A, Scanell J W and Young M P 2000 *Phil. Trans. R. Soc. B* **355** 91
- [31] Segev R, Benveniste M, Shapira Y and Ben-Jacob E 2003 *Phys. Rev. Lett.* **90** 168101
- [32] Volman V, Baruchi I and Ben-Jacob E 2005 *Phys. Biol.* **2** 98
- [33] Zhou C, Zemanová L, Zamora-López G, Hilgetag C C and Kurths J 2007 *New J. Phys.* **9** 178
- [34] Rulkov N F 2001 *Phys. Rev. Lett.* **86** 183
- [35] Rulkov N F 2002 *Phys. Rev. E* **65** 041922
- [36] Chialvo D R and Apkarian A V 1993 *J. Stat. Phys.* **70** 375
- [37] Gao Z, Hu B and Hu G 2001 *Phys. Rev. E* **65** 016209
- [38] Perc M and Gosak M 2008 *New J. Phys.* **10** 053008
- [39] Volman V and Levine H 2009 *Chaos* **19** 033107
- [40] Tinsley M, Cui J, Chirila F V, Taylor A, Zhong S and Showalter K 2005 *Phys. Rev. Lett.* **95** 038306
- [41] Lu Q, Gu H, Yang Z, Shi X, Duan L and Zheng Y 2008 *Acta. Mech. Sin.* **24** 593
- [42] Connors B W and Long M A 2004 *Annu. Rev. Neurosci.* **27** 393
- [43] Perotti J I, Billoni O V, Tamarit F A, Chialvo D R and Cannas S A 2009 *Phys. Rev. Lett.* **103** 108701